

BOND GRAPH PROPORTIONAL-INTEGRAL OBSERVER-BASED ROBUST FAULT DETECTION

Ghada Saoudi ^(a), Rafika El Harabi ^(b), Geneviève Dauphin-Tanguy ^(c), Belkacem Ould Bouamama ^(d), Mohamed Naceur Abdelkrim ^(e)

^(a) ECOLE NATIONALE D'INGENIEURS DE GABES, TUNISIE

^(b) ECOLE NATIONALE D'INGENIEURS DE GABES, TUNISIE

^(c) ECOLE CENTRALE DE LILLE, FRANCE

^(d) POLYTECH' LILLE, FRANCE

^(e) ECOLE NATIONALE D'INGENIEURS DE GABES, TUNISIE

^(a) saoudighada90@hotmail.fr, ^(b) rafikaharabi@yahoo.fr, ^(c) genevieve.dauphin-tanguy@ec-lille.fr,

^(d) belkacem.ouldbouamama@polytech-lille.fr, ^(e) naceur.abdelkrim@enig.rnu.tn

ABSTRACT

The present paper investigates a bond graph tool to design full-order proportional-integral (PI) observers for a robust fault detection purpose. The proposed method allows the calculation of the gain matrix graphically through covering causal paths and loops based on the pole placement techniques for linear systems. The robust residuals are further generated from an uncertain bond graph model in linear fractional transformation (LFT) form so as to detect actuator faults in presence of parameter uncertainties. Simulation tests on a hydraulic system show the dynamic behavior of system variables and the robustness of the PI observers in the presence of modeling errors. The effectiveness of the proposed robust fault detection estimator is later illustrated via a DC motor.

Keywords: Bond Graph, Proportional-Integral observer, Robust fault detection, Linear fractional transformation, DC motor

1. INTRODUCTION

Bond graph approach has been developed in recent years as a powerful tool for modeling dynamical systems. It essentially focuses on the exchange of energies between the system and its environment and between different elements within the system.

Robust fault diagnosis has been the subject of several researches, due to the increase of system complexity, and the industrial requirement around the safety and the yield (Isermann 1993). In this context, due to the structural and causal properties of quantitative graphical approaches, the bond graph is more and more used for modeling and fault diagnosis. Bond graph representation can be used for monitoring ability (i.e. ability to detect and to isolate faults) and supervision system's design via the generation of formal Analytical Redundancy Relations (ARRs) in a systematic way (Djeziri, Merzouki, Ould Bouamama

and Dauphin Tanguy 2007). In his works, Djeziri dealt with the generation of fault indicators in the presence of parameter uncertainties by using a bond graph representation in linear fractional transformation (LFT) form. Since diagnosis using (ARRs) is more common in practice, in this paper we will particularly focus the attention on the design of graphical PI observers for robust fault detection issue.

For the general case of systems modeled by the bond graph tool, little has so far been achieved in the development of associated FDI graphical observers. Abderrahmène (Sallami, Zanzouri and Ksouri 2012) integrated a method of robust diagnosis based on observers for systems with parameter uncertainties modeled by the bond graph. Hence, the observer design is obtained by using graphical methods and referring to structural properties (Sueur and Dauphin Tanguy 1989).

For this reason, the main interest of the present paper is to build a robust bond graph observer (RBGO) in proportional-integral form (Pichardo-Almarza, Rahmani, Dauphin-Tanguy and Delgado 2003) for linear systems based on causal and structural properties for graphical approach (Bond Graph). It consists to generate residual signals from linear BG-LFT models to take into account the presence of parameter uncertainties in multiplicative form.

The outline of the paper is as follows: Section 2 presents the graphical PI observers design for linear systems while section 3 deals with the robust residual generation. Illustrative examples of a hydraulic system and a DC motor are developed in section 4 and show the efficiency of the proposed robust fault detection estimator.

2. DESIGN OF A GRAPHICAL PI OBSERVER

2.1. Conventional PI observer

The Luenberger observer is itself a linear dynamic system. Its input values are the values of measured

outputs from the original system, and its state vector generates missing information about the state of the original system. The observer can be regarded as a dynamic device that, when connected to the available system outputs, generates the entire state. However, the idea of a proportional integral observer, Fig.1, is to use additionally the integral of the error as follows:

$$\hat{w} = \int_0^t (y(\tau) - C\hat{x}(\tau))d\tau \quad (1)$$

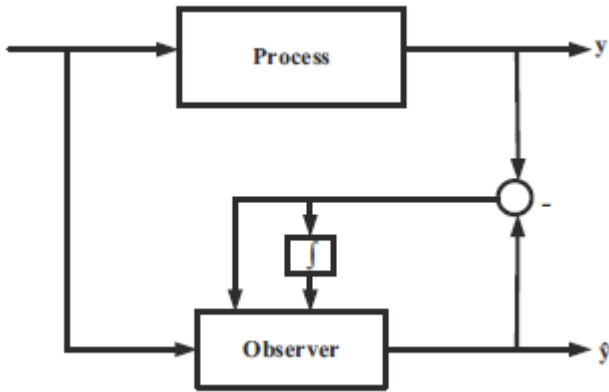


Figure 1: Proportional Integral Observer's diagram.

Then, the PI observer for the model is written using this set of equations:

$$\begin{cases} \frac{d\hat{x}}{dt} = A\hat{x} + Bu + K_p(y - C\hat{x}) + K_I\hat{w} \\ \frac{d\hat{w}}{dt} = y - C\hat{x} \end{cases} \quad (2)$$

where x in \mathcal{R}_n , y in \mathcal{R}_q , and u in \mathcal{R}_m are respectively the state, the measurement output and the control input vectors. A , B and C are constant matrices of proper dimensions. K_I and K_p are respectively the integral and proportional gains. Hence, the error equation ($e_x = \hat{x}$ and $e_w = \hat{w}$) is defined as:

$$\begin{pmatrix} \frac{de_x}{dt} \\ \frac{de_w}{dt} \end{pmatrix} = \begin{pmatrix} A - K_p C & -K_I \\ C & 0 \end{pmatrix} \begin{pmatrix} e_x \\ e_w \end{pmatrix} \quad (3)$$

2.1.1. Bond Graph PI observer

The algorithm presented in this section is dedicated to fault detection observers for linear systems, in which bond graph tool is used.

- **Step 1: Checking the existence of any redundant outputs** The existence of redundant outputs is the first condition to check for the observer construction. The interest of this step is to avoid unnecessary calculations. Indeed, the selection of the non-redundant outputs allows the computing of the gain K with minimal size. This condition can be verified by calculating the rank of the observation matrix C (difference between the number of detectors D_e and D_f , and the detectors which cannot be dualized in the bond graph in integral causality).

- **Step 2: Checking the structural observability of the model**

Property 1: From a Bond Graph point of view proposed by Sueur and Dauphin-Tanguy (Sueur and Dauphin Tanguy 1989) a bond graph model is structurally observable if and only if the following conditions are met:

1. On the bond Graph model in integral causality, there is a causal path between all the dynamic elements I and C and a detector D_e or D_f . Or,
2. All dynamic elements admit a derivative causality in the derivative bond graph model. If there are dynamic elements remaining in integral causality, the dualization of detectors D_e and D_f is necessary.

- **Step 3: Construction of the Luenberger bond graph observer** The objective of this stage is to design the BGO equivalent to the conventional Luenberger observer equation defined as:

$$\begin{cases} \dot{x} = Ax + Bu + K(y - \hat{y}) \\ \hat{y} = C\hat{x} \end{cases} \quad (4)$$

The BGO is composed of the integral bond graph model to which the term $K(y - \hat{y})$ is added. Figures 2 and 3 represent the linear output injection in the dynamic components I and C , by using modulated flow sources for an element I and modulated effort sources for an element C .

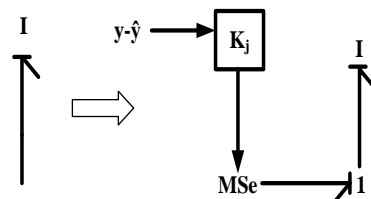


Figure 2: Linear output injection: case of an I element.

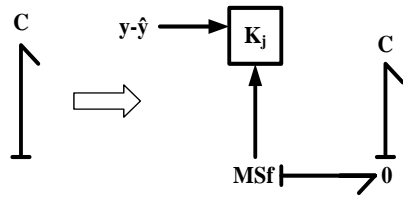


Figure 3: Linear output injection: case of a C element.

- Step 4: Construction of the bond graph PI observer** The Bond Graph model is defined with the changes described in the below figures. In the same way, modulated effort sources (respectively flow sources) are used when the state variable is associated with an I-element (respectively a C-element) to apply the integral action in the observer.

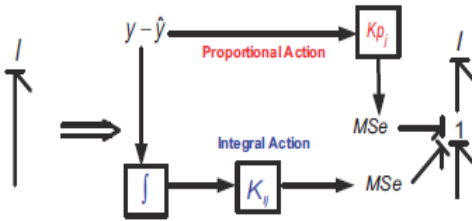


Figure 4: Linear output injection: case of an I element.

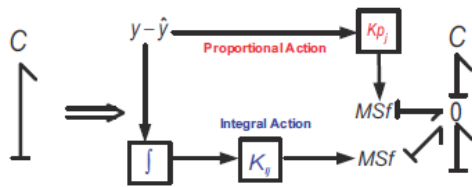


Figure 5: Linear output injection: case of a C element.

3. ROBUST RESIDUAL GENERATION

Inspired from BG-LFT representation introduced by (Dauphin and Djeziri 2006), graphical PI observers are used to generate robust residual signals by following these steps:

- Verify that the uncertain bond graph model in LFT form of the system is reachable and structurally observable;
- Construction of the BG PI observer;
- The residual signal (residual output estimation) is deduced from this equation: $r = y - \hat{y}$.

In the next section, we will illustrate the effectiveness and the performance of the developed graphical PI estimator comparing to Luenberger one (Saoudi, EL Harabi and Abdelkrim 2012; Saoudi, EL Harabi and Abdelkrim 2013) via a hydraulic system with two tanks. Robust fault residuals are tested through a DC motor with parameter uncertainties under multiplicative form.

4. SIMULATION AND DISCUSSIONS

4.1. Hydraulic System with two tanks

Consider the sketch of the studied system where its characteristic values are presented in Table 1. From the bond Graph model in integral causality (see Figure 7), the associated graphical PI observer is deduced verifying these steps:

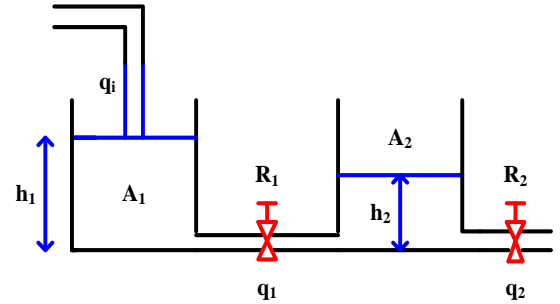


Figure 6: Hydraulic system with two tanks.

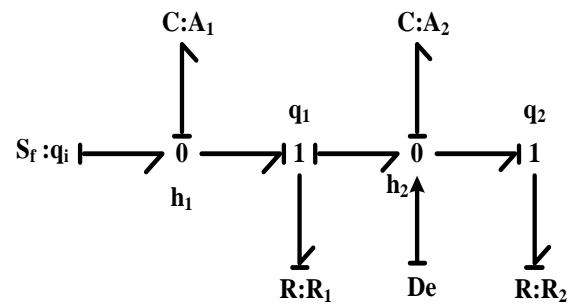


Figure 7: Bond Graph model of the system in integral causality.

Table 1: Parameter Values

Elements		
Parameter	Symbol	Value
Section Area of tank 1	A_1	1m^2
Section Area of tank 2	A_2	2m^2
Hydraulic Resistance 1	R_1	$10\text{m}(\text{m}^2\text{s}^{-1})^{-1}$
Hydraulic Resistance 2	R_2	$20\text{m}(\text{m}^2\text{s}^{-1})^{-1}$

- Step 1: Checking the existence of redundant outputs.** This step is unnecessary in this case study, since the model has only a single detector.
- Step 2: Verification of the structural observability.** As it is mentioned previously, the structural observability, can be easily obtained using structural analysis of the derivative bond graph model (DBG) (See

Figure 8). All the dynamic elements admit a derivative causality; hence, the model is structurally observable.

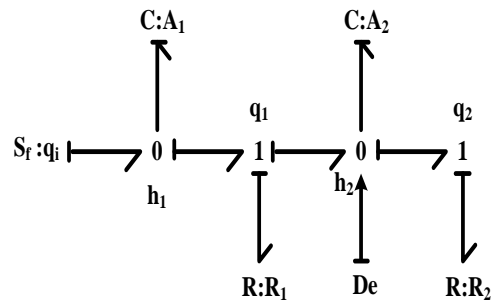


Figure 8: Bond Graph model in derivative causality.

- **Step 3: Construction of the Luenberger BG observer.** It is possible to construct a Luenberger observer from the bond graph model by using linear output injection cited above.

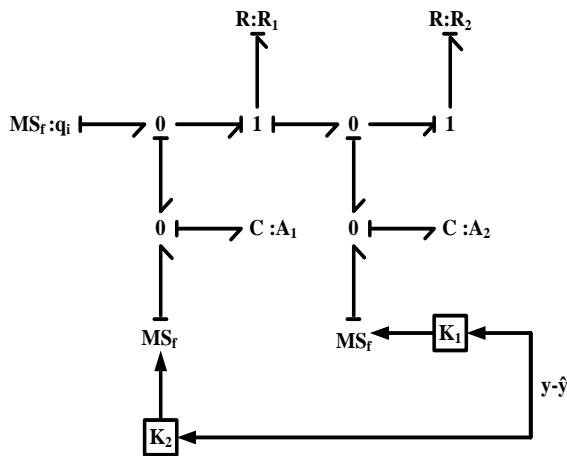


Figure 9: Bond Graph model of the Luenberger observer.

- **Step 4: Construction of the PI observer-based bond graph (BGO).** The proposed BG PI observer is described in Fig.10 after modifying the bond graph model.

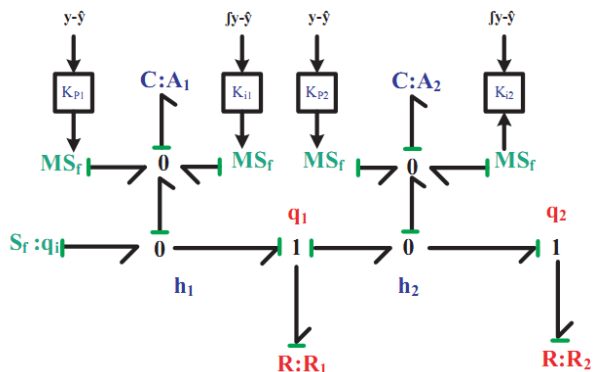


Figure 10: Bond graph model of the graphical PI observer.

- **Step 5: Gain calculation of the BG PI observer.** We calculate Kp as the gain of the Luenberger observer. We choose the poles of the observer and such that they are slightly faster than the poles of the model and non-oscillating.

$$s = \begin{bmatrix} s_1 \\ s_2 \end{bmatrix} = \begin{bmatrix} -0.318 \\ -0.032 \end{bmatrix} \quad (5)$$

This selection gives the following desired characteristic polynomial:

$$P_d(s) = s^2 + 0.35s + 0.01 \quad (6)$$

with these coefficients and after the calculation of causal cycles of order 1-2, we obtain Kp as

$$Kp = \begin{bmatrix} 2 \\ 0.15 \end{bmatrix} \quad (7)$$

Then, we can apply the same method to calculate KI using the calculated values of KP for the Luenberger observer, with the following poles selection:

$$s = \begin{bmatrix} -0.318 \\ -0.032 \\ -0.0033 \end{bmatrix} \quad (8)$$

Furthermore, the desired polynomial for the PI observer is:

$$P_d(s) = s^3 + 0.3533s^2 + 0.1115s + 0.00003 \quad (9)$$

with these coefficients, we obtain now three equations depending on the components of K1 and KP. We use the values of Kp2 calculated for the Luenberger observer and after the calculation of the family of causal cycles of order 1-3, we can calculate the new Kp1 and K1 vector that generate the coefficients of the desired polynomial.

Finally, we obtain the following gains:

$$Kp = \begin{bmatrix} Kp_1 \\ Kp_2 \end{bmatrix} = \begin{bmatrix} -0.2467 \\ 0.15 \end{bmatrix} \quad (10)$$

$$K_I = \begin{bmatrix} K_{I1} \\ K_{I2} \end{bmatrix} = \begin{bmatrix} 0.00373 \\ -0.00718 \end{bmatrix} \quad (11)$$

The initial conditions of the BG model states in integral causality are considered null. Simulation tests were implemented in 20-sim software. In this part, The performance of the Luenberger and PI observers are evaluated in presence of modeling errors. Thus, let's consider that the hydraulic resistance parameter R2 for

the OBG have a variation of -10% in comparison with the parameters of the BG model.

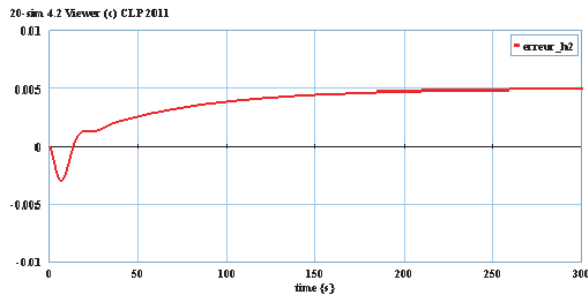


Figure 11: Estimation error via the Luenberger BG observer.

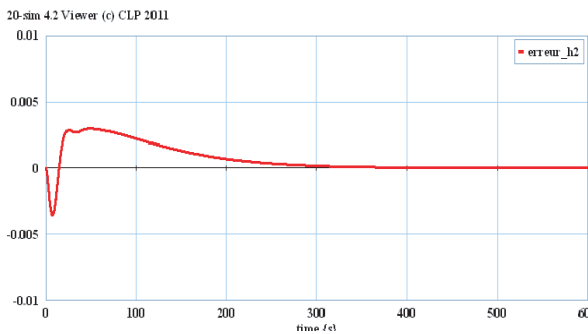


Figure 12: Estimation error via the BG PI observer.

We conclude that the estimation error converges to zero despite the presence of modeling errors in the observer's parameters unlike to the graphical Luenberger observer (see figures 11 and 12).

Now, Let's use the BG PI observer for a robust fault detection purpose.

4.2. DC motor

The DC motor is a combination of electrical and mechanical fields. The electrical part corresponds to an RL circuit. It is composed of an input voltage source U_{alim} , an electrical inductance L_a and an electromotive force feedback represented by a gyrator (GY) (with a constant k). The mechanical part is characterized by a rotor inertia J , a viscous friction parameter b and transmission axle rigidity.

The nominal characteristics and parameter values of the DC motor are defined in Tables 2 and 3.

Table 2: Nominal Operation Of The Dc Motor

DC Motor Characteristics	
Power	1KW
Velocity (w)	452tr/mn
Current (I_a)	1.8A
Voltage (U_{alim})	47.3V

Table 3: Parameter and Uncertainties Values Of The DC Motor

Parameter and Uncertainties Values			
Symbol	Parameter	Value	Uncertainty
R_a	Armature Resistance	8Ω	0
L_a	Rotor Inductance	0.129 H	$\delta_{L_a}=0.0002$
k	Constant Torque	0.07745	0
J	Constant Inertia	0.02Kg.m ²	$\delta_J=0.00035$
b	Fluid Friction	0.0218 Nm/s	0

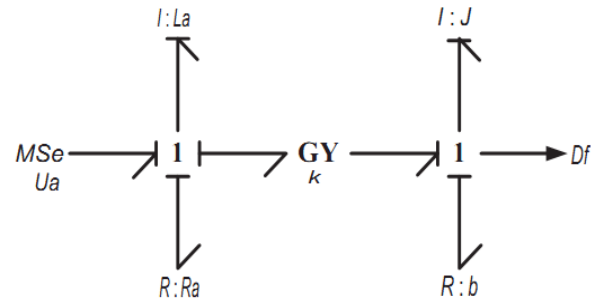


Figure 13: Bond graph model of the DC motor with permanent magnet.

To this bond graph model of the DC motor (see Fig.13), we will apply the method described in section 2 in order to design the graphical PI observer.

The bond graph model of the studied system (see Fig.14) is structurally observable (steps 1 and 2 are verified).

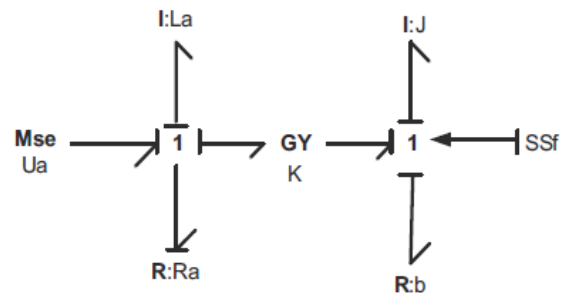


Figure 14: Bond graph model in derivative causality.

- **Step 3: Construction of the Luenberger BG observer.** The bond graph model of the proportional observer is deduced as seen in Fig.15.

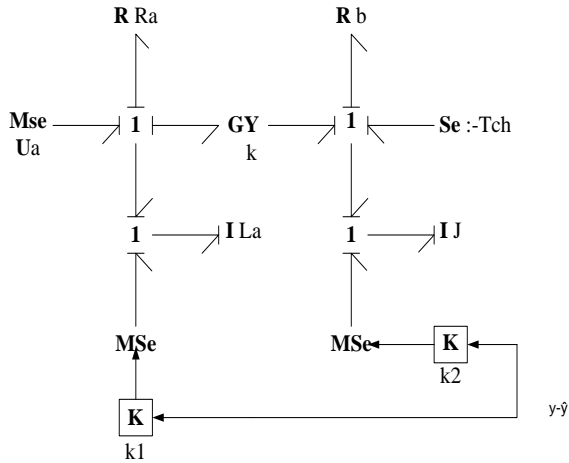


Figure 15: Bond graph model of the Luenberger observer.

- **Step 4: Construction of the BG PI observer.** PI observer deduced from BG model is presented in Fig.16.

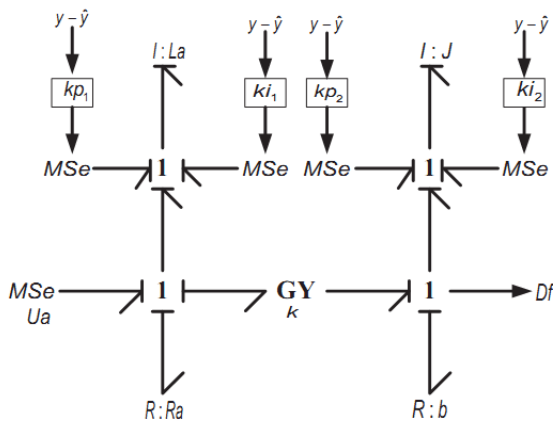


Figure 16: Bond graph model of the PI observer.

- **Step 5: Calculation of the observer gain (K_P and K_I).** It is determined using the bond graph models of the observers. Applying the same technique to calculate the gains of the previous observer, from Fig.16 we obtain the corresponding families of causal cycles (see Table 4).

a_i	Causal Cycle families	Gains
β_1	$I:L_a \leftarrow 1 \rightarrow R:Ra$	$G_a = (-1) \cdot \frac{-R_a}{L_a s}$
	$I:J \leftarrow 1 \rightarrow R:b$	$G_b = (-1) \cdot \frac{-b}{J s}$
	$J \uparrow \leftarrow 1 \leftarrow MSe \leftarrow \boxed{K_{p2}} \leftarrow y - \hat{y}$	$G_c = (-1) \cdot \frac{-k_{p2}}{J s}$
β_2	$I:L_a \uparrow \leftarrow 1 \leftarrow GY_k \leftarrow 1 \leftarrow I:J$	$G_d = (-1) \cdot \frac{-k^2}{L_a J s}$
	$y - \hat{y} \downarrow \leftarrow \boxed{K_{p1}} \rightarrow MSe \rightarrow 1 \leftarrow 1 \rightarrow GY_k \rightarrow 1 \leftarrow J \uparrow$	$G_e = (-1) \cdot \frac{-k \cdot k_{p1}}{L_a J s^2}$
	$J \uparrow \leftarrow 1 \leftarrow MSe \leftarrow \boxed{K_{i2}} \leftarrow y - \hat{y}$	$G_f = (-1) \cdot \frac{-k_{i2}}{J s^2}$
	$J \leftarrow 1 \rightarrow b$ $L_a \leftarrow 1 \rightarrow R_a$	$G_g = \frac{R_a \cdot b}{L_a J s^2}$
	$L_a \leftarrow 1 \rightarrow R_a$ $J \uparrow \leftarrow 1 \leftarrow \boxed{K_{p2}} \leftarrow y - \hat{y}$	$G_h = \frac{R_a \cdot k_{p2}}{L_a J s^2}$
	β_3	$L_a \uparrow \leftarrow \boxed{K_{i1}} \leftarrow y - \hat{y}$ $1 \leftarrow MSe \leftarrow 1 \leftarrow GY_k \leftarrow 1 \leftarrow J \downarrow$
$L_a \leftarrow 1 \rightarrow R_a$ $J \uparrow \leftarrow 1 \leftarrow \boxed{K_{i2}} \leftarrow y - \hat{y}$ $1 \leftarrow MSe$		$G_j = \frac{k_{i2} \cdot R_a}{L_a J s^3}$

Finally, we obtain the following gains:

$$K_p = \begin{bmatrix} 2.3 \\ 0.3642 \end{bmatrix} \quad (11)$$

$$K_I = \begin{bmatrix} -5.217 \\ 10.998 \end{bmatrix}$$

The input signal U_{alim} and the load torque T_{ch} , in normal situation, are illustrated respectively in figures 18 and 19. Moreover, the estimated states $i_{a_{est}}$ and w_{est} when a PI observer is used are shown in figures 20 and 21. The observer error is near zero. In this case, it is able to estimate states. Thus, the obtained estimator can be used to generate residual signals.

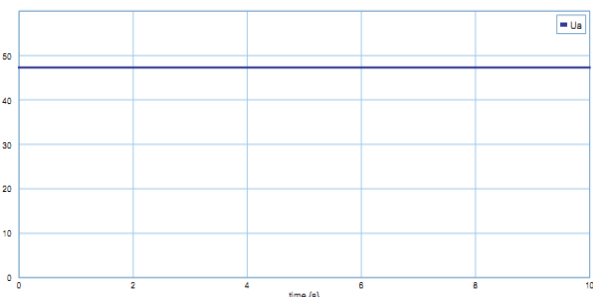


Figure 18: Input signal evolution.

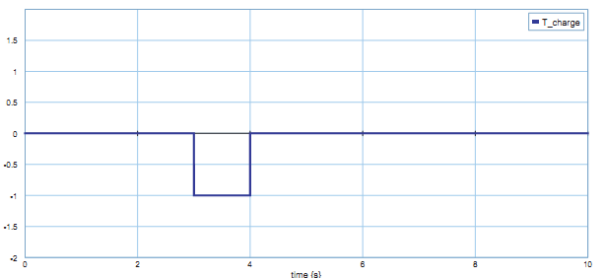


Figure 19: Load torque evolution.

The figures 20 and 21 show a clear precision of estimation of the systems state variables. We observe, also, that the pace of the estimated variables $i_{a_{est}}$ and w_{est} and the state variables i_a and w are indistinguishable.

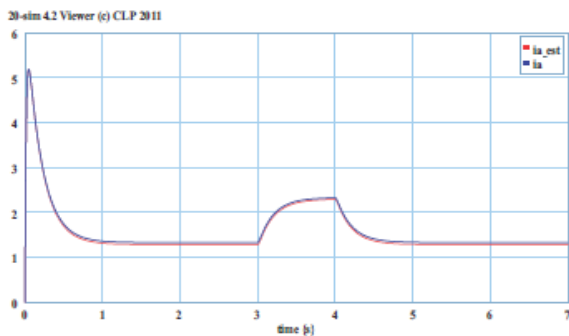


Figure 20: Estimation of the Induced current via the BG PI observer.

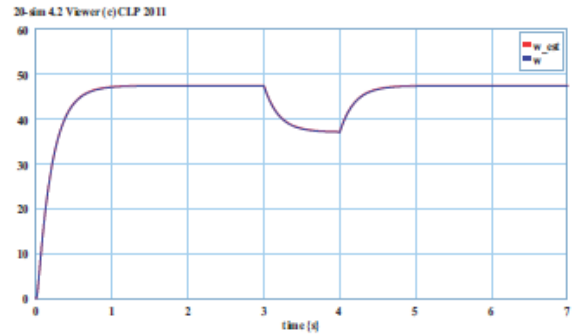


Figure 21: Estimation of the velocity via the BG PI observer.

The estimation errors are null as it is shown in figures Fig.23 and Fig.24.

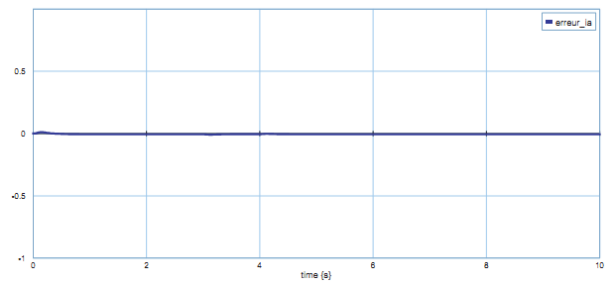


Figure 22: Estimation error of the induced current.

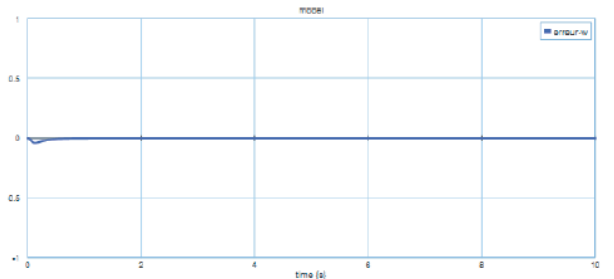


Figure 23: Estimation error of the velocity.

In LFT bond graph representation, parameters uncertainties are represented under multiplicative form at the level of bond graph component, which represent respectively, the inertia J and the rotor inductance L_a in the DC motor. The graphical linear PI observer is depicted in Fig.24. Indeed, the proportional-integral observer provides a more robust estimation against parameter uncertainties as it is shown in figures 25 and 26. The estimation errors are practically null. Thus, the robustness of the graphical PI observer against modeling errors.

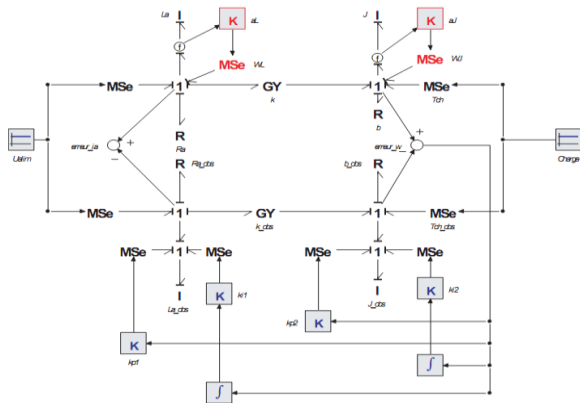


Figure 24: BG-LFT model with multiplicative uncertainties of the system and its observer.

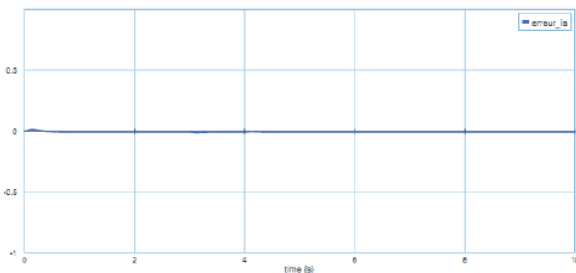


Figure 25: Estimation error of the induced current in faulty free case (in presence of parameter uncertainties).

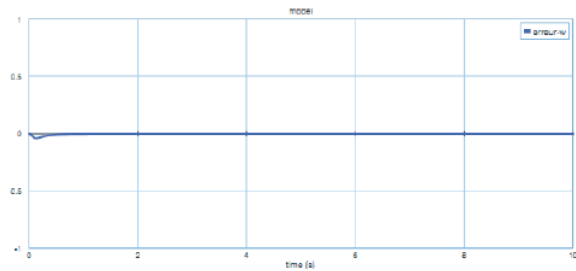


Figure 26: Estimation error of the velocity in faulty free case (in presence of parameter uncertainties).

Hence, it improves the performance and the efficiency of the bond graph PI observer. Now, it can be used to generate fault indicators.

However, DC motor failures can be classified as electrical and mechanical faults and the residues are obtained from the linear graphical PI observer.

The fault scenario considers the occurrence of the actuator fault (partial blocked rotor), with subtractive amplitude of 20 Volt between the instants 3s and 4s (abrupt failure), while the motor is operating in charge.

From figures 27 and 28, we observe that the state variables are affected by the occurrence of this default and drawn aside from their nominal values.

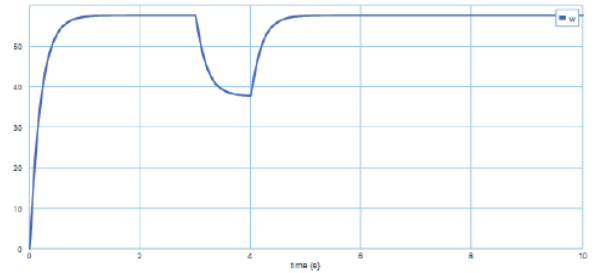


Figure 27: Velocity evolution in faulty case.

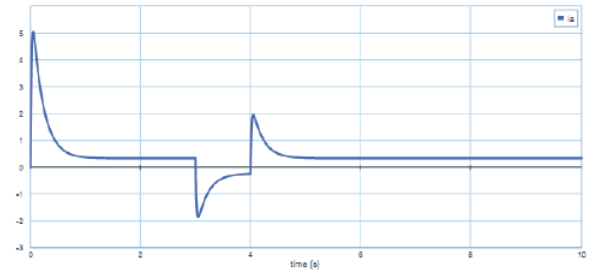


Figure 28: Induced current evolution in faulty case.

Figures 29 and 30 show that residues are different from zero during the appearance of the actuator failure. Then, the graphical PI observer able guarantee a robustness to parameter uncertainties and a sensitivity against faults.

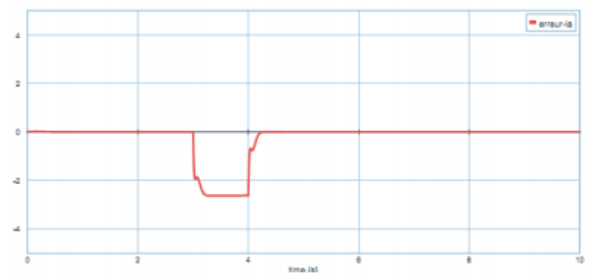


Figure 29: Residual response in abnormal situation (r_1).

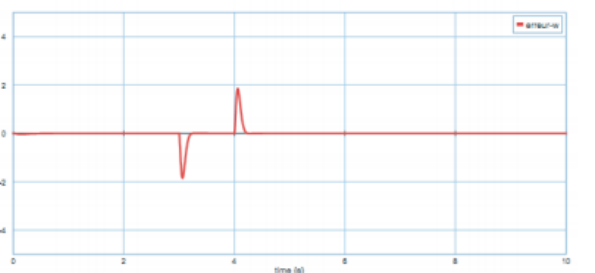


Figure 30: Residual response in abnormal situation (r_2).

5. CONCLUSION

In this paper, a robust fault detection procedure using a proportional-integral observer based on bond graph model for linear systems has been addressed. This approach is based exclusively on the causal handling operated on a bond graph representation. The

implementation of graphical PI observers improve the residual generation. In fact, the obtained fault indicators are robust to the multiplicative parameter uncertainties and the modeling errors. The major interest of this approach lies in the fact that the bond graph model has a true physical direction and gives access to many flow and effort variables. Due to graphical proportional-integral observer's limits, future works will focus on an unknown input observer design so as to ensure more robustness against disturbances.

REFERENCES

- Isermann, R., 1993. Fault diagnosis of machines via parameter estimation and knowledge processing. *Automatica*, 29 (4), 815–836.
- Djeziri, M., Merzouki, R., Ould Bouamama, B., Dauphin-Tanguy, G., 2007. Robust Fault Diagnosis by Using Bond Graph Approach. *IEEE Transactions on Mechatronics*, 12 (6).
- Luenberger, D., 1966. Observers for multivariable systems. *IEEE Transactions on Automatic Control*, 11, 190–197.
- Karnopp, D., 1979. Bond Graphs in Control: Physical State Variables and Observers. *Journal of The Franklin Institute*, 308 (3), 221–234.
- Pichardo-Almarza, C., Rahmani, A., Dauphin-Tanguy, G., Delgado, G., 2003. Bond Graph Approach to Build Reduced Order Observers in Linear Time Invariant Systems. *Proceedings of 4th MATHMOD, Fourth International Symposium on Mathematical Modeling*.
- Hajji, N., Rahmani, A., 2010. Observer for an omnidirectional mobile robot. *ICBGM*, Orlando: USA.
- Loureiro, R., BenMoussa, S., 2011. Graphical approach for state reconstruction and monitoring analysis. *The 5th International Conference on Integrated Modeling and Analysis in Applied Control and Automation IMAACA*, Rome: Italy, 259–266.
- Sallami, A., Zanzouri, N., Ksouri, M., 2012. Robust Fault Diagnosis Observer of Dynamical Systems Modelled by Bond Graph Approach. *International Journal of Computer Science and Network Security*, 12 (1).
- Sueur, C., Dauphin-Tanguy, G., 1989. Structural Controllability and Observability of linear Systems Represented by Bond Graphs. *Journal of Franklin Institute*, 326, 869–883.
- EL Harabi, R., Ould Bouamama, B., El Koni Ben Gayed, M., Abdelkrim, M., 2012. Bond graphs for diagnosis of chemical processes. *Computers & chemical engineering*, 36, 301–324.
- EL Harabi, R., Ould Bouamama, B., El Koni Ben Gayed, M., Abdelkrim, M., 2011. Bond Graph Model Based for Robust Fault Diagnosis. *Computers & chemical engineering. the 5th International Conference on Integrated Modeling and Analysis in Applied Control and Automation IMAACA*, Rome: Italy, 259–266.
- Beale, S., Shafai, B., 1989. Robust control System Design with a proportional integral observer. *International Journal of Control*, 50 (1), 97–11.
- Busawon, K., Kabore, P., 2000. On the design of integral observers and proportional integral observers. *Proceedings of the American Control Conference*, 3275–3279.
- Saoudi, G., EL Harabi, R., Abdelkrim, M., 2012. Fault Detection Based on Luenberger Observers. *CRATT*, Tunis: Tunisia.
- Saoudi, G., EL Harabi, R., Abdelkrim, M., 2013. Graphical Linear Observers For Fault Detection. *SSD*, Hammamet: Tunisia.
- El Harabi, R., 2011. *Supervision des Processus Chimiques à Base de Modeles Bond Graph*. Thesis (PhD). Gabes University.
- Rahmani, A., 1993. *Etude structurelle des systèmes linéaires par l'approche bond graph*. Thesis (PhD). Lille University.